AD-A069 083 NAVAL RESEARCH LAB WASHINGTON DC F/G 20/5
ABLATIVE ACCELERATION OF LASER-IRRADIATED THIN FOIL TARGETS.(U)
MAR 79 R DECOSTE, S E BODNER, B H RIPIN

UNCLASSIFIED NRL-MR-3948 SBIE-AD-E000 297 NL

1 OF 1
AD A069 083

END
DATE FILMED
7-79
DDC

NRL Memorandum Report 3948

Ablative Acceleration of Laser-Irradiated Thin Foil Targets

R. DECOSTE, S.E. BODNER, B.H. RIPIN, E.A. MCLEAN,
S.P. OBENSCHAIN, AND C.M. ARMSTRONG

Plasma Physics Division

March 9, 1979

NAVAL RESEARCH LABORATORY
Washington, D.C.

SECURITY CLASSIFICATION OF THIS PAGE (When Data Entered)

REPORT DOCUMENTATION PAGE		READ INSTRUCTIONS BEFORE COMPLETING FORM
1. REPORT NUMBER NRL Memorandum Report 3948	2. GOVT ACCESSION NO.	3. RECIPIENT'S CATALOG NUMBER
4. TITLE (and Subtitle) ABLATIVE ACCELERATION OF LASER-IRRADIATED THIN FOIL TARGETS*		5. TYPE OF REPORT & PERIOD COVERED Continuing 6. PERFORMING ORG. REPORT NUMBER
7. AUTHOR(s) R. Decoste[a], S. E. Bodner, B. H. Ripin, E. A. McLean, S. P. Obenschain[a], and C. M. Armstrong[b]		8. CONTRACT OR GRANT NUMBER(s)
9. PERFORMING ORGANIZATION NAME AND ADDRESS Naval Research Laboratory Washington, D.C. 20375		10. PROGRAM ELEMENT, PROJECT, TASK AREA & WORK UNIT NUMBERS 67H02-29A
11. CONTROLLING OFFICE NAME AND ADDRESS Department of Energy Washington, D.C. 20545		12. REPORT DATE March 9, 1979 13. NUMBER OF PAGES 11
14. MONITORING AGENCY NAME & ADDRESS(if different from Controlling Office)		15. SECURITY CLASS. (of this report) Unclassified 15a. DECLASSIFICATION/DOWNGRADING SCHEDULE

16. DISTRIBUTION STATEMENT (of this Report)

Approved for public release; distribution unlimited

17. DISTRIBUTION STATEMENT (of the abstract entered in Block 20, if different from Report)

18. SUPPLEMENTARY NOTES

*Work sponsored by the U.S. Department of Energy

a. Sachs/Freeman Associates, Bladensburg, MD

b. North Carolina State University, Raleigh, NC

19. KEY WORDS (Continue on reverse side if necessary and identify by block number)

Laser-Fusion
Ablation
Foil Acceleration
Ion Expansion

(10 to the 12 power - 10 to the 13th power W/sq cm)

20. ABSTRACT (Continue on reverse side if necessary and identify by block number)

Ablative acceleration of thin foil targets at low laser irradiance (10^{12}-10^{13} W/cm^2) are studied experimentally and theoretically. Ablative acceleration of foils up to ~ 10^7 cm/sec with good hydrodynamic efficiency (20%) have been achieved. These and other results are in good agreement with a simple rocket model.

approximately 10 to the 7th power

DD FORM 1 JAN 73 1473 EDITION OF 1 NOV 65 IS OBSOLETE
S/N 0102-014-6601

SECURITY CLASSIFICATION OF THIS PAGE (When Data Entered)

ABLATIVE ACCELERATION OF LASER-IRRADIATED THIN FOIL TARGETS

In the laser fusion concept, the near-isentropic implosion of the pellet fuel is driven by the rocket-like ablation of the pellet shell. Pellet design considerations suggest that acceleration of the shell to a velocity of $\sim 2 \times 10^7$ cm/sec is sufficient.[1] We demonstrate, here, ablative acceleration of thin foil targets to velocities of $\sim 1 \times 10^7$ cm/sec with good hydrodynamic efficiency ($\sim$20%). Most aspects of ablation physics can be studied most easily with thin planar foils rather than pellets.[2] The laser intensity at 1.06μm is chosen at or below 10^{14}W/cm^2 to maximize the ablation efficiency and laser light absorption. An array of small calorimeters and time-of-flight particle detectors surround the target to measure ablation variables. The structure and behavior of the rear target surface is also studied with several optical diagnostics, to confirm the acceleration and to provide information about the spatial and velocity distributions across the accelerating target. The hydrodynamic behavior is found to be consistent with a simple analytical model.

In this paper, we compare our results to a simple model which treats the one-dimensional ablative acceleration of the target analogously to that of a rocket. During the acceleration phase, the target (rocket) with mass M and velocity v is accelerated by the steady-state blowoff (exhaust) of the ablated plasma (propellant) at a constant velocity u in the target reference frame (Fig. 1a), i.e., $Mdv/dt = -udM/dt$. This relation is integrated to yield the well-known rocket equation,[3]

$$v/u = \ln(M_o/M), \tag{1}$$

Manuscript submitted January 11, 1979.

where M_o is the initial target mass. The hydrodynamic efficiency η_h is defined as the directed energy of the accelerated foil divided by the absorbed laser energy, i.e., $\eta_h = \frac{1}{2}Mv^2/E_a$. Using Eq. (1) and the fact that the rate of absorbed laser energy must be balanced by the energy dissipated in the ablation and acceleration of the target (neglecting radiative losses), we obtain

$$\eta_h = \frac{(v/u)^2}{\exp(v/u)-1.} \tag{2}$$

For small fractional mass loss, these equations reduce simply to

$$\eta_h \simeq v/u \simeq \Delta M/M_o, \tag{3}$$

where $\Delta M = M_o - M$. Note that these equations contain no explicit assumptions about heat transport or density and temperature profiles.[4,5] This information is lumped into a knowledge of the ion ablation velocity u, to be experimentally determined. It has also been shown that the steady-state assumption is indeed valid after $\sim$1 nsec for *Nd* - laser pulses.[6]

Equations (1) and (2), relating the ablation variables, are plotted in Fig. 2b (solid lines). When the target velocity becomes comparable to the ablation velocity, the hydrodynamic efficiency increases to a maximum of 65%, where 80% of the initial mass is ablated.[7] However, the data presented below is obtained for cases where Eq. (3) applies, i.e., for $u/v > 1$.

The ablation pressure (thrust) P_a exerted on the target (rocket) by ablation, for a one-dimensional ablation, is given by mdv/dt, where m is a mass per unit area. This yields the relation

$$P_a = 2I_a/u, \tag{4}$$

where I_a is the effective absorbed laser flux. For the laser fusion application, an important consideration is to optimize the hydrodynamic efficiency by varying the pressure or irradiance. Pellet design considerations fix a well-defined relationship between η_h and P_a for a given laser

wavelength. Figure 1b shows a hypothetical example. As the laser flux decreases, the ablation pressure drops and the efficiency (and thus pellet gain) increases. Since the shell aspect ratio $R/\Delta R$, is inversely proportional to P_a, there is a lower limit to the pressure, given by the Rayleigh-Taylor instability (dashed line). Our experiments are a first attempt to find that optimal point for 1.06 μm radiation which maximizes efficiency with acceptable stability.

Several diagnostics are used in these studies to measure the ablation and acceleration properties required for a comparison with the model. Thin foil targets are irradiated at $0.3-1\times10^{13}$W/cm^2 through an aspheric $f/10$, 1-meter lens by locating the target several millimeters out of best focus towards the lens, thereby increasing the irradiated area and uniformity of illumination. Both the spatial and temporal focal distributions are known over 4 decades in intensity.[2] Laser light absorption exceeds 80% as measured with a box calorimeter and discrete minicalorimeters.[2] Figure 2*a* is a typical example of ablative acceleration data with a 15-μm thick *CH* foil at 10^{13}W/cm^2. The angular distributions of the ion energy and velocity on the laser side, and the accelerated target material, are measured with the minicalorimeters and time-of-flight detectors. The time-of-flight detectors exhibit the single narrow velocity distributions characteristic of ablation[4] (on the laser side) and accelerated target. The observed average ion ablation velocity u (3.3×10^7cm/sec, averaged over all angles on the laser side), and the final average target velocity (5.1×10^6cm/sec) are consistent with results using the optical diagnostics discussed below. The hydrodynamic efficiency η_h (6.6%) is directly obtained from the integration of the angular energy distributions. Finally, the fraction of the mass ablated (0.25) is inferred from the proper angular integration of the energy divided by the square of the velocity.

The ablated mass and velocity are mostly a function of irradiance and pulse duration. Therefore, it is possible to control the fraction of the mass ablated, and obtain different values for the final target velocities and hydrodynamic efficiencies, by varying only the initial foil

thickness. These experimental results are shown in Fig. 2b, together with a comparison with the rocket model. The dashed line in Fig. 2b is a correction introduced in the one-dimensional model to account for the experimentally observed effective ion blowoff angle of 40° to the target normal. Only the target motion and the momentum transferred normal to the target surface are compared in this model. The high absorption fraction of the incident laser light (80%), combined with the efficient ($\leqslant$20%) ablative accelerion to high velocity ($\sim 10^7$ cm/sec) observed so far, at these irradiances, is encouraging.

The ablation pressures inferred from Eq. (4) are respectively 1 and 3 Mbars, for the 450- and 230-μm laser spot size cases (irradiances of 3×10^{12} and 1×10^{13} W/cm^2) and thick foils. Edge effects become important when thin targets are accelerated a distance comparable to the laser spot diameter. In this case, the laser energy flows towards the side as well as towards the accelerated target. Edge effects are experimentally observed as an increase in the effective diameter of ablated material beyond the laser spot size with a corresponding decrease in the penetration depth of the thermal wave into the material. It should be emphasized, however, that the scaling between the ablation variables is still valid even when the ablated thickness of material becomes foil thickness dependent. More details about measurements of edge effects, lateral and axial heat transport in general are described in Ref. 2.

Some of the structure and behavior of the rear surface of the foil[8] obtained during the acceleration phase with optical diagnostics are shown in Fig. 3. Figure 3a shows three edge-view shadowgram frames, taken with a short-duration probe beam ($\sim$400 psec, 5320 $\AA$) at different times with respect to the peak of the main laser pulse. From a series of shadowgrams, the displacement and, consequently, the velocity of the rear surface is obtained as a function of time. Velocity data from frame and streak shadowgraphy, as well as an asymptotic velocity obtained from Fig. 2 are compared in Fig. 3b. The streak shadowgraphy data is obtained using

the non-shortened 5320 Å probing beam as a backlighting source. The smooth and continuous acceleration of the rear surface seen in Fig. 3b ($\sim 10^{15}$cm/sec^2) is consistent with the applied pressure inferred from Eq. (4), and can not be easily explained by other phenomena such as shock wave or spallation. The Doppler shift, and thus velocity of the cold rear surface of the target is measured by imaging the short-duration probe light reflected from the rear target surface onto the entrance slit of a stigmatic spectrograph. Figure 3c shows the Doppler inferred velocity profiles at times - 0.8 nsec and +0.2 nsec relative to the peak of the main laser pulse for a 7-μm thick Al target. At the later time, a slug of material comparable to the laser spot size has apparently broken away from the rest of the target and is accelerated to a nearly spatially uniform velocity of $\sim 10^6$ cm/sec, consistent with the model.

To conclude, it has been shown that in the long pulse, low irradiance regime considered here, thin foil targets can be ablatively accelerated up to $\sim 10^7$ cm/sec with good hydrodynamic efficiency ($\sim$20 %). These results are in reasonable agreement with the simple analogy to a rocket and are encouraging for the laser fusion application. Future experiments will deal more fully with laser beam uniformity requirements and the stability of the accelerated foils.

The authors gratefully acknowledge the contributions of J. Boris, S.H. Gold, J. Grun, J.A. Stamper, R.R. Whitlock and F.C. Young. This work is sponsored by the U.S. Dept. of Energy.

REFERENCES

(a) Present association: Sachs/Freeman Associates, Bladensburg, Md.

(b) Present association: North Carolina State University, Raleigh, NC.

1. D. Henderson, private communication (1977); J.H. Nuckolls et al., European Conf. on Laser Inter. with Matter, Oxford, England (1977) (unpublished).

2. For a detailed discussion see: NRL Laser-Plasma Interaction Group, NRL Memo Report No. 3890, ed. B. H. Ripin (Dec. 1978). Also, B. H. Ripin et al. (to be published).

3. R. Resnick and D. Holliday, "Physics," Vol. I, 3rd ed., pg. 178, J. Wiley, NY (1978).

4. K.A. Brueckner and S. Jorna, Rev. Mod. Phys, 46, 325 (1974); T.R. Jorboe, W.B. Kunkel, A.F. Lietzke, Phys. Fluids 19, 1501 (1976); F.S. Felber, Phys. Rev. Lett. 29, 84 (1977); S.J. Gitomer, R.L. Morse and B.S. Newberger, Phys. Fluids 20, 234 (1977).

5. J.P. Anthes, M.A. Gusinow and M.K. Matzen, Phys. Rev. Lett. 41, 1300 (1978); M.A. Gusinow, J.P. Anthes, M.K. Matzen and D. Woodall, Appl. Phys. Lett. 33, 800 (1978).

6. M.K. Matzen and R.L. Morse, Bull. Am. Phys. Soc. 23, 787 (1978).

7. F.S. Felber, Nucl. Fusion 18, 1469 (1978).

8. N.G. Kovalskij, M.T. Pergament and P.P. Pashinin, presented at IAEA Meeting, San Francisco, CA (Jan. 1978) (unpublished).

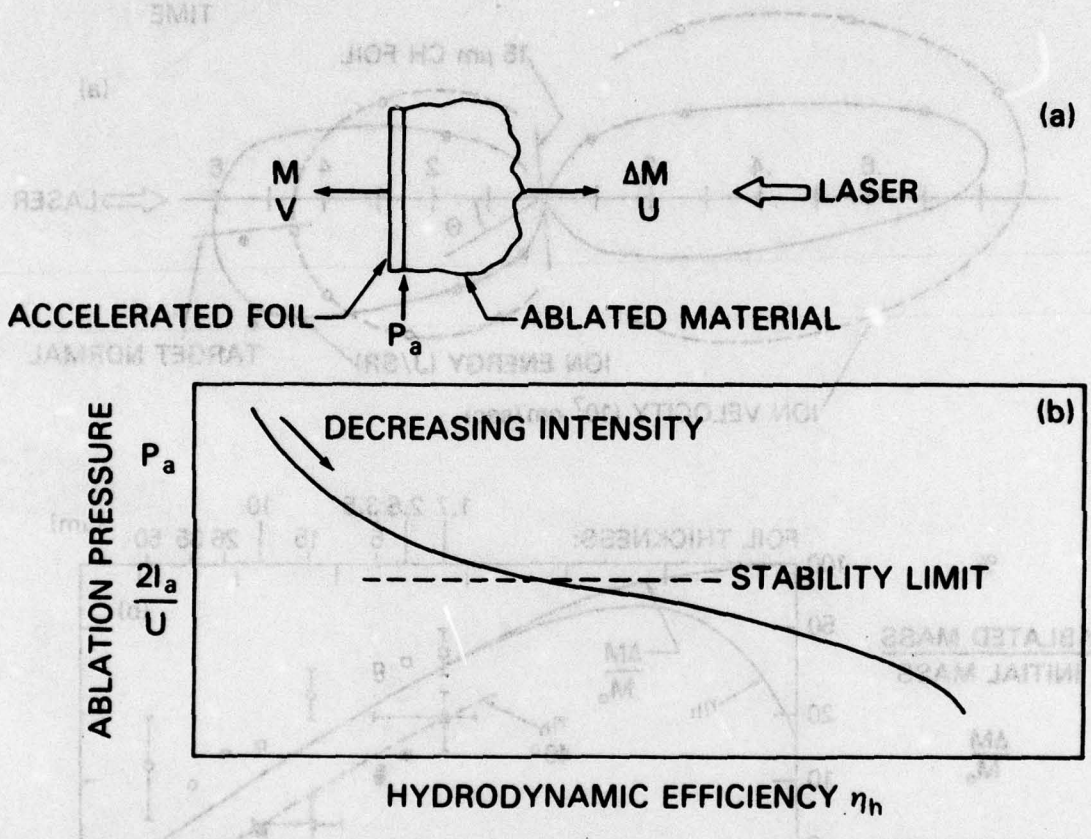

Fig. 1 — (a) Ablative acceleration of thin foils. The ion ablation velocity u is defined in the accelerated foil frame. (b) Schematic relationship between ablation pressure and hydrodynamic efficiency. Targets can be stably accelerated above the dashed line.

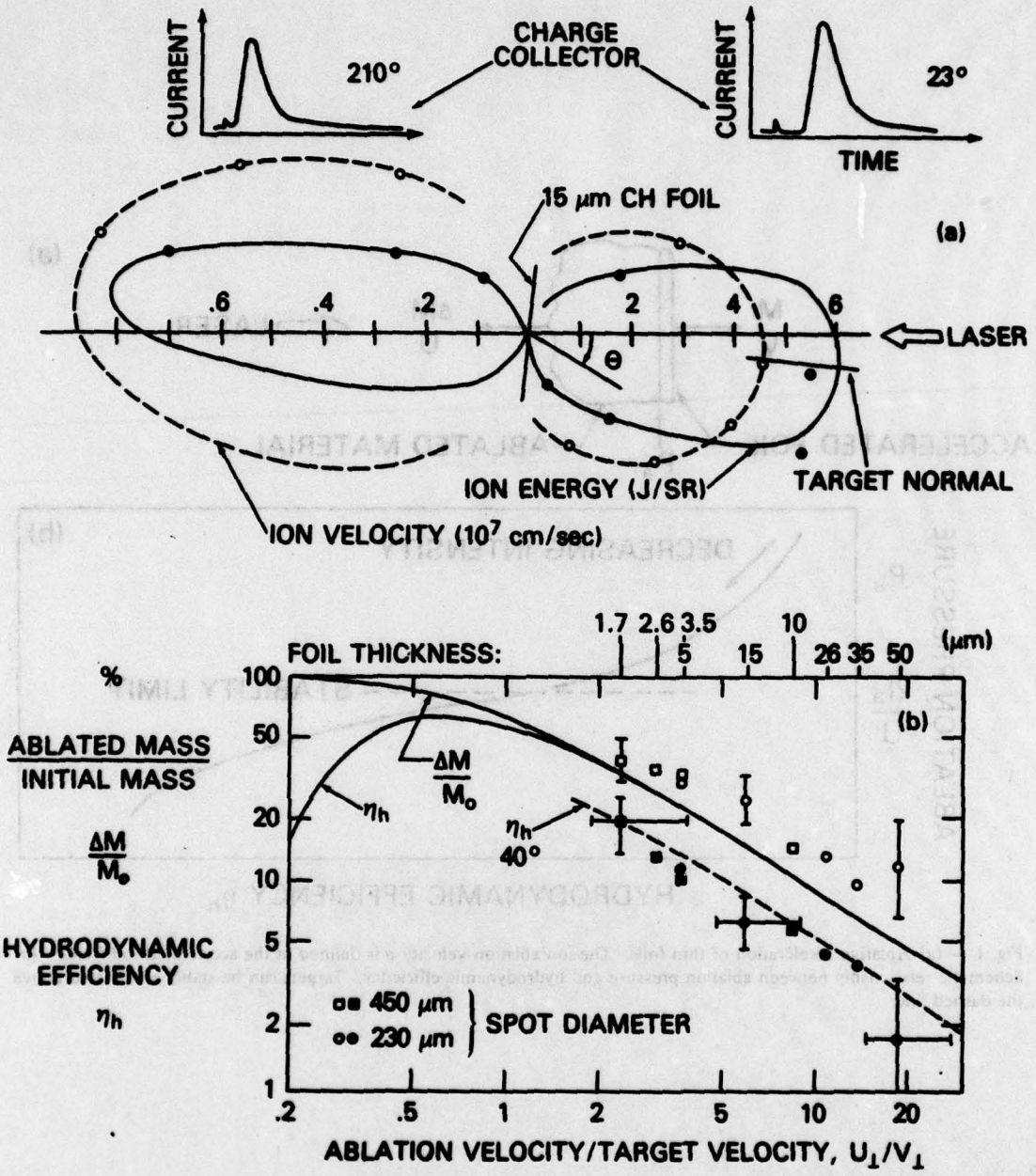

Fig. 2 (a) Typical ablative acceleration data. The average ion ablation velocity u, the final target velocity v, the hydrodynamic efficiency η_h and the mass fraction ablated $\Delta M/M_o$ are inferred from the angular distributions of energy and velocity. Note the change of scales on the rear versus the front. For this example the *Nd* -laser parameters were 1×10^{13} W/cm^2 over a 230-μ m spot diameter for 3 nsec (FWHM). (b) Ablative acceleration: comparison of experiment and model. Black and open data points correspond respectively to η_h and $\Delta M/M_o$. Experiments were done with varying foil thickness and spot diameters. The error bars are the larger of either standard deviation or estimated measurement uncertainties.

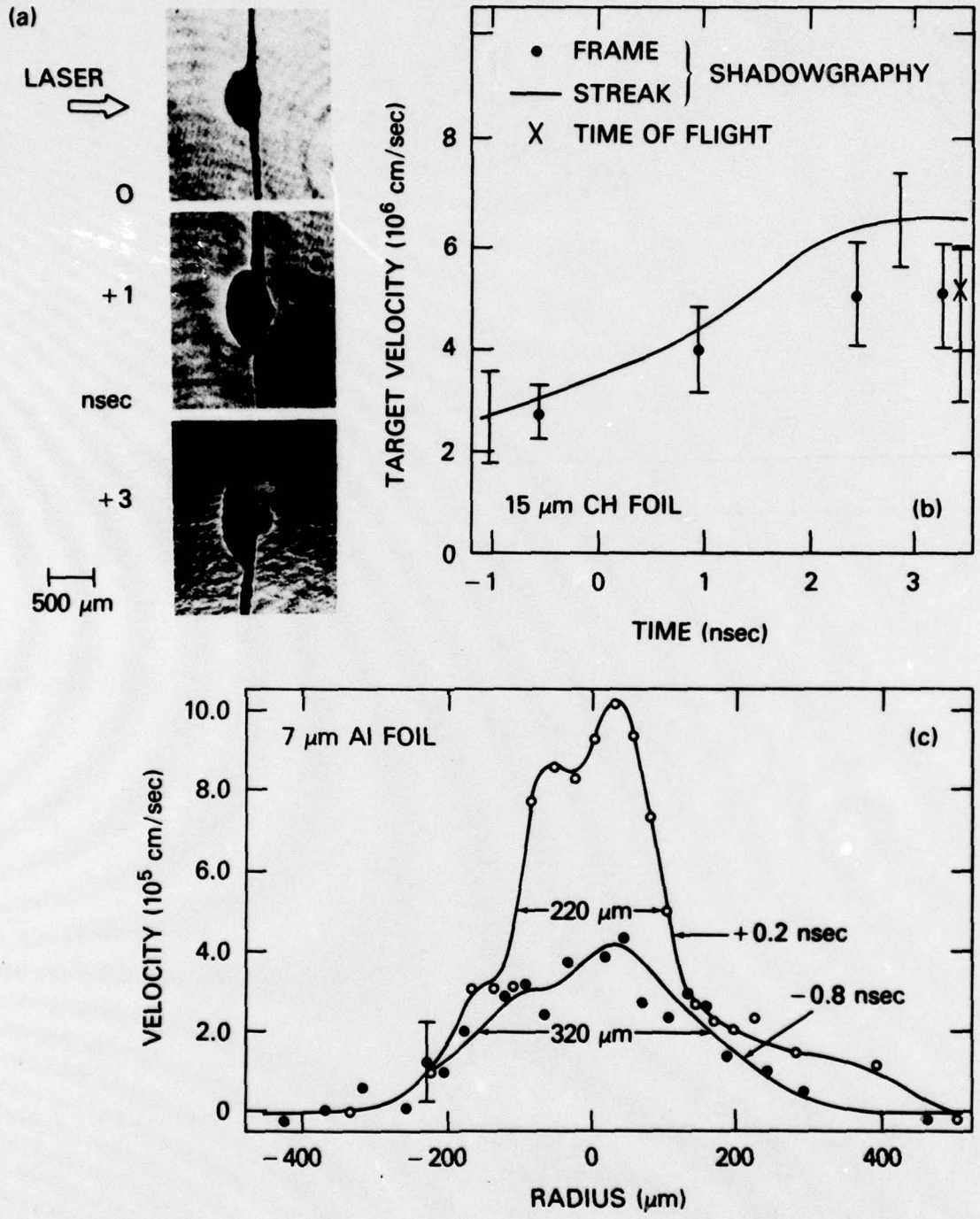

Fig. 3 — Dynamic of ablatively accelerated targets. (a) Frame shadowgrams of irradiated *CH* foils at selected times with respect to the peak of the laser pulse. (b) Rear surface velocity versus time obtained with streak (solid line) and frame (black circles) shadowgraphy, and asymptotic time-of-flight velocity determination. (c) Doppler-shift velocity profiles across the rear surface of a 7-μm *Al* target for the same laser parameters as in (b) above and Fig. 2a. Note that the FWHM of the velocity profile at +0.2 ns is equal to the laser spot size within experimental accuracy.